# Roles of grain boundary and dislocations at different deformation stages of nanocrystalline copper under tension

Y.G. Zheng [a], H.W. Zhang [a,*], Z. Chen [a,b], C. Lu [c], Y.-W. Mai [d]

[a] *State Key Laboratory of Structure Analysis for Industrial Equipment, Department of Engineering Mechanics, Dalian University of Technology, Dalian 116024, P. R. China*

[b] *Department of Civil and Environmental Engineering, University of Missouri, Columbia, Missouri 65211-2200, USA*

[c] *Department of Mechanical Engineering, Curtin University of Technology, Perth, WA 6845, Australia*

[d] *Centre for Advanced Materials Technology (CAMT), School of Aerospace, Mechanical and Mechatronic Engineering J07, The University of Sydney, Sydney, NSW 2006, Australia*

## ABSTRACT

The plastic deformation of nanocrystalline copper subjected to tension has been studied using molecular dynamics simulation. The results show that, in the initial stage, the deformation is mainly boundary-mediated in small grains; while in the late stage, the deformation is accommodated by dislocations in large grains. It is also found that the stress-assisted grain growth occurs owing to atomic diffusion and grain boundary migration. These results are consistent with recent experimental observations.

*PACS*: 62.25.+g; 61.82.Bg; 47.11.Mn

*Keywords*: Nanocrystalline copper; Molecular dynamics simulation; Plastic deformation; Dislocation; Grain growth

* E-mail address: zhanghw@dlut.edu.cn

Nanocrystalline (nc) materials have been widely studied over the past two decades owing to their outstanding physical, mechanical and chemical properties such as high strength, good thermal stability, enhanced diffusivity, and thermal conductivity [1–3]. nc materials include single- and multi-phase polycrystals with grain sizes of 1–250 nm and a large volume fraction of atoms being located in the grain boundary (GB) area. Experimental observations and computer simulations have shown that the properties of nc materials are closely tied to their peculiar microstructures and unique deformation mechanisms. It is of great importance to understand the structure–property relationships in materials down to the nanometer range that have attractive potential for advanced applications in nanoscale devices [2].

The plastic deformation of conventional coarse-grained materials is mainly accommodated by dislocation nucleation and motion. However, this mechanism and its corresponding models break down when applied to nc materials. To fully understand the mechanical response of an nc material to external loading, many efforts have been devoted to uncover the underlying physics, including experimental studies, fundamental theoretical analyses, and advanced computer simulations. For example, mechanical milling tests showed that the formation and migration of partial disclination dipoles allow nanostructured iron to fragment and rotate during severe plastic deformation [4]. Deformation twinning [5,6], another mechanism that accommodates plastic deformation in nc aluminium and copper, is thought to be directly related to the particular nanostructures, which has not been observed in their coarse-grained counterparts. The grain boundary-mediated process becomes a prominent deformation mode in these materials as the grain size decreases to tens of nanometers [5–7]. Recently, several theoretical models have been proposed to explain the rotational plastic deformation and dislocation nucleation mechanism experimentally observed in nanomaterials [8,9]. Although experimental observations have exhibited a completely different picture of deformation at

nano-scales, the atomic details of deformation cannot be obtained owing to the limitations of current experimental facilities.

Molecular dynamics (MD) plays an increasingly important role in exploring the details of atomic motion and structural evolution in nc materials, and in understanding the underlying deformation mechanisms [10]. MD simulations on the deformation of nc copper showed a softening phenomenon with the decrease of grain size, i.e., the reverse Hall-Petch effect, owing to a large fraction of atoms at the GBs [11]. Two distinct atomic processes, atomic shuffling and stress-assisted free-volume migration, have been revealed on the GBs during sliding [12,13]. Coble-creep was found at the smallest grain size, which means that GB sliding is the predominant deformation mechanism [10]. In addition, by using a <110> -textured microstructure of hexagonal, same-sized grains, it has been detected that a partial dislocation was emitted from a GB, traveled through the entire grain, and ultimately absorbed by the opposite GBs [14]. Trailing partials in some materials like aluminium follow after the emission of leading partials; while in other materials like copper, a trailing partial was not seen but a stacking fault (SF) defect transecting the entire grain was formed [15]. Some details of dislocation-dislocation and dislocation-twin interactions were also revealed by computer simulations [16]. It seems that GB-mediated deformation, such as GB sliding and grain rotation, is responsible for plastic deformation in small grains (< 10 nm), while dislocation-accommodated plastic deformation mainly occurs in grains with a relatively large size (> 30 nm) [10–17].

Although significant advancement in the understanding of mechanical deformation of nc materials has been made, the following two important problems are still not fully understood: (1) What are the predominant mechanisms at different deformation stages of nc materials subjected to mechanical loads? (2) How can grain growth in an nc system be facilitated by the

presence of high stress? In this letter, we take face-centered cubic (fcc) copper as an example to investigate the deformation mechanisms of nc materials under uniaxial tension, with a focus on the difference between GB-mediated and dislocation-based mechanisms. Using the MD approach, the atomic details of these two mechanisms and their competition (or interplay) are studied.

In single-phase materials, grain size distributions usually follow a log-normal function and the average number of grain faces is ~6 (or ~14) in a two- (or three-) dimensional system [18]. Here, let us consider a three-dimensional, columnar nc copper sample. To represent a more realistic microstructure, the initial *xy*-plane profile of the sample is generated using a modified Potts model combined with Monte Carlo (MC) procedure [19,20], as shown in Fig. 1. The grain sizes lie in a relatively large range and follow a log-normal distribution, with textured orientation in the $z$ ($<1\bar{1}0>$) direction and randomly chosen mis-orientation angles (≥ 15°) between two adjacent grains. Individual grains are filled with copper atoms that occupy the fcc lattice with a specified orientation. The sample contains 184,325 atoms in 14 grains with diameters of 6–18 nm, corresponding to a system size of 44.5×38.6×1.28 $nm^3$. Initially, the system is annealed at 300 K to obtain a stress-free equilibrium structure. Then, a uniaxial strain rate of $4\times10^8$ $s^{-1}$ is applied along the $x$-axis, keeping the stresses along the $y$- and $z$-axis zero. Periodic boundary conditions are applied in all directions. During the loading process, the temperature is kept at 300 K using a Nosé-Hoover thermostat [21,22]. The embedded atom method (EAM) [23] is used in the MD simulations. The stacking fault energy and unstable stacking fault energy given by the EAM are 17.2 and 157.8 $mJ/m^2$, respectively, and the unstable twin fault energy is 166.9 $mJ/m^2$ [24]. The equations of motion are integrated with time using a velocity Verlet algorithm [25]. The local atomic structures are determined by the Voronoi construction and are used to identify the dislocation core, SF, and deformation

twin [26].

A typical tensile stress-strain curve is shown in Fig. 2. It can be seen that, when uniaxial strain is less than ~2.5%, the stress is approximately a linear function of strain, i.e., elastic deformation is dominant. Despite the high loading rate used in MD simulations, it is worth noting that Young's modulus of nc copper that was estimated to be about 105 GPa approaches the experimental value of 120 GPa [11]. When the critical strain is larger than 2.5%, the stress is roughly unchanged but with small fluctuations and the flow stress is ~2.1 GPa. The corresponding microstructure evolution during tensile loading is also shown in the insets of Fig. 2. In the early stage, the sample undergoes mainly elastic deformation so that dislocations and SFs are seldom observed [see inset (a)]. Then, as accompanied with the nucleation and propagation of several partial dislocations, plastic deformation starts [see inset (b)]. With further increase of loading, more and more dislocations appear and a dense network of SFs forms. As a result, the sample undergoes severe plastic deformation [from insets (c) to (f)]. The SF density, however, changes very slowly in the late stage [see insets (g) and (h)].

During the plastic deformation process, atoms adjacent to GBs slip on the most close-packed plane subjected to external loading or diffusion and re-arrange near the triple junction of GBs, inducing relative sliding between two neighboring grains because of their different slip systems. Thus, grain rotation occurs as a result of cooperative sliding along the opposite boundaries of the grain. Figure 3 shows the in-plane rotation angles of five selected grains with different diameters as a function of time. It is obvious that small grains rotate much faster than large ones. For example, after 500 ps, the magnitude of in-plane rotation angle of grain 7 (with diameter $D_7$ = 6.7 nm) is about 30°, while it is about 10° for grain 2 with a larger diameter of $D_2$ = 17.4 nm. It is interesting to note that there are several distinct rotation stages in the process (see Fig. 3): (1) during elastic deformation, almost all grains do not rotate; (2)

in the early stage of plastic deformation, the rotation rate of small grains is relatively high but the rotation of large grains is still not evident; and (3) after ~12% of applied strain is reached, the rotation rate of small grains decreases while large grains tend to rotate fast.

Besides the GB sliding-induced grain rotation, the plastic deformation of nc copper is also accommodated by the nucleation, propagation and interaction of dislocations. Two types of dislocation motions are commonly observed: (1) the single partial dislocation motion where a partial dislocation of $1/6[\bar{1}1\bar{2}]$ nucleates from the GB, propagates into the interior of a grain and is eventually absorbed by the opposite GB, leaving behind a SF transecting the grain; and (2) the extended dislocation motion where two partials connected by a SF emit in sequence from the GB, move inside the grain, and are ultimately absorbed by the opposite GB. The partial is found in all grains of the simulated sample; while the extended dislocation is only observed in large grains because the distance between two partials is inversely proportional to the stacking fault energy and because a larger interior space is needed for its formation [10]. It is worth noting that, even in large copper grains, an extended dislocation can only be formed after a relatively long simulation time (~400 ps) because of the low temperature and large energy barrier between stable and unstable SFs [15]. During their motion in a large grain, two partial dislocation cores may meet and interact with each other. They can induce the formation of the Cottrell-Lomer lock. If the motion planes of these partial cores are the same or parallel, they can separate the intrinsic stacking fault and transform the extrinsic stacking fault to twin. Since the energy for a trail partial nucleation is comparable to that for a twin fault formation in nc copper, thus, both extended dislocation and deformation twin are observed in simulations [15].

As discussed above, there are two kinds of mechanisms which accommodate the plastic deformation of nc copper, i.e., grain boundary-mediated and dislocation-based ones. These

two mechanisms operate in different grains and stages: the former dominates in small grains and at an early plastic deformation stage, and the latter primarily controls the deformation of large grains at a late stage. During tensile loading, however, they co-exist and interplay with each other. Grain boundary sliding and rotation can facilitate the formation of dislocations. In nano-structured materials, dislocation cores are usually formed near GBs. This is because the local atomic structure of GBs is so disordered that the displacement misfit may be introduced into the system in a deformation process and a relative glide of atoms induces the formation of cores. Conversely, dislocation-based deformation can affect GB sliding and grain rotation, i.e., deformation twin and Cottrell-Lomer lock can induce two-fold (both stimulative and suppressive) effects on the GB-mediated process [16]. Deformation twins facilitate plastic deformation by adding extra slip systems. Once formed, these twins can repel certain types of gliding dislocations because their crystallographic axes are different on both sides. This suppressive mechanism makes the local structure stable in a certain period. The Cottrell-Lomer locks, formed by the interaction between dislocations, also inhibit sliding of certain atoms as deformation twins. It is the interplay between these two mechanisms that directly results in three distinct deformation and rotation stages (see Figs. 2 and 3). In the elastic stage, because the stress is too low to trigger GB sliding, the rotation is not activated and almost all the grains are kept unchanged. In the early stage of plastic deformation, the rotation rate is relatively high and the sample undergoes severe plastic deformation owing to the GB sliding-induced grain rotation and the formation and motion of dislocations. In the later stage, the rotation rate decreases to a low level owing to the occurrence of some suppressive ingredients, such as deformation twins and Cottrell-Lomer locks formed by the interaction of dislocations, which inhibit the atoms gliding in certain close-packed planes and decrease the rotation rate of small grains. These results are consistent with recent

experimental observations in the tensile test of nc alloys [27].

In conventional materials, the Hall-Petch effect (hardness and yield strength increase with decreasing grain size) is generally observed. However, this effect often ceases to exist or even reverses in nc materials. There is a transition from the dislocation-based mechanism to the GB-mediated mechanism. The GBs can improve hardness and yield strength by serving as an inhibitor in coarse-grained materials to deter the generation and motion of dislocations inside a grain. However, they act as sources for dislocation nucleation and atom sliding to facilitate the plastic deformation in nc materials. Although the deformation transition from small grains to large ones appears during the loading process, it does not make much difference in the stress-strain curve (see Fig. 2) because grain rotation and dislocation nucleation originate from the motion of boundary atoms. The transition size in nc copper is about 10–20 nm. This differs from the conventional observation of strain-softening of coarse-grained materials where dislocations initiate in the interior of a grain. It is the interplay and competition between these two kinds of mechanisms that may be responsible for the super-plasticity as observed in our simulations.

During the loading process, the atoms adjacent to GBs diffuse from one grain to another, leading to grain growth or shrinkage. In addition, the GB could migrate as a whole under stress, which also facilitates the grain growth. Figure 4 shows the shrinkage of grain 8 by virtue of the boundary migration, accompanying by the growth of its neighboring grains 2, 3, 7 and 10. The initial size of grain 8 is ~8.2 nm. After 12% of applied strain (i.e., 300 ps), the grain size decreases to ~4.0 nm. Usually, thermally activated grain growth proceeds as a time scale of seconds, and is difficult at low temperature [28]. However, it is found that, in MD simulations, the grain growth occurs in a very short time period despite the high loading rate. This rapid growth suggests that the process is stress-assisted, which is consistent with recent

experimental and computational results from the indentation test of nc copper [28,29] and the tensile test of polycrystal nickel nanowire [30]. Generally, most small grains shrink during loading (grains 6 and 8). However, some small ones like grain 7 grow rather than consumed by large grains. This may be due to their local environments that are assembled by some peculiar short-length GBs with relatively low mis-orientation angles. Hence, the network effect is operative that prevents the contraction of these small grains. After 20% of applied strain, the total number of grains decreases to 12 (grains 6 and 8 merged with others), i.e., the average grain size increases from the initial diameter of ~12.5 nm to ~13.5 nm. However, it should be pointed out that the current study is inadequate in giving a statistical description of the kinetics of stress-assisted grain growth in the system owing to the limitation of the number of grains used in MD simulations.

In summary, the deformation mechanism in an nc-fcc copper system has been investigated using the MD method. It is found that the GB-mediated deformation is mainly responsible for small grains during loading, while the dislocation-based mechanism commonly exists in large grains. Atomistic details show that the interplay and competition between these two mechanisms induce two distinct plastic deformation stages. In the early stage, GB sliding together with the rotation of small grains is dominant and partials emit from the GB with SFs behind. These SFs then transect small grains. With further loading, extended dislocations can be formed in large grains and the rotation of small grains is suppressed by the formation of the Cottrell-Lomer locks and deformation twins. MD simulation has also shown that grain growth is triggered by high stresses. These results are consistent with experimental observations and provide a better understanding of the plastic deformation and other unusual mechanical properties of nc materials.

**Acknowledgments**

This work was supported by the National Natural Science Foundation of China (10721062, 90715037, 10728205), the Program for Changjiang Scholars and Innovative Research Team in University of China (PCSIRT), the 111 Project (B08014), and the National Key Basic Research Special Foundation of China (2005CB321704). CL and YWM acknowledge the support from the Curtin Internal Research Grant and the Australian Research Council (ARC), respectively.

**References**

[1] H. Gleiter, Prog. Mater. Sci. 33 (1989) 223.

[2] M.A. Meyers, A. Mishra, D.J. Benson, Prog. Mater. Sci. 51 (2006) 427.

[3] C. Lu, Y.-W. Mai, Y.G. Shen, J. Mater. Sci. 41 (2006) 937.

[4] M. Murayama, J.M. Howe, H. Hidaka, S. Takaki, Science 295 (2002) 2433.

[5] M.W. Chen, E. Ma, K.J. Hemker, H.W. Sheng, Y.M. Wang, X.M. Cheng, Science 300 (2003) 1275.

[6] X.Z. Liao, Y.H. Zhao, S.G. Srinivasan, Y.T. Zhu, R.Z. Valiev, D.V. Gunderov, Appl. Phys. Lett. 84 (2004) 592.

[7] Z.W. Shan, E.A. Stach, J.M.K. Wiezorek, J.A. Knapp, D.M. Follstaedt, S.X. Mao, Science 305 (2004) 654.

[8] M.Y. Gutkin, I.A. Ovid'ko, Appl. Phys. Lett. 87 (2005) 251916.

[9] M.Y. Gutkin, I.A. Ovid'ko, Appl. Phys. Lett. 88 (2006) 211901.

[10] D. Wolf, V. Yamakov, S.R. Phillpot, A. Mukherjee, H. Gleiter, Acta Mater. 53 (2005) 1.

[11] J. Schiotz, F.D. Di Tolla, K.W. Jacobsen, Nature 391 (1998) 561.

[12] H. Van Swygenhoven, M. Spaczer, A. Caro, D. Farkas, Phys. Rev. B 60 (1999) 22.

[13] H. Van Swygenhoven, P.M. Derlet, Phys. Rev. B 64 (2001) 224105.

[14] V. Yamakov, D. Wolf, M. Salazar, S.R. Phillpot, H. Gleiter, Acta Mater. 49 (2001) 2713.

[15] H. Van Swygenhoven, P.M. Derlet, A.G. Froseth, Acta Mater. 54 (2006) 1975.

[16] V. Yamakov, D. Wolf, S.R. Phillpot, H. Gleiter, Acta Mater. 51 (2003) 4134.

[17] F. Sansoz, J.F. Molinari, Acta Mater. 53 (2005) 1931.

[18] H.V. Atkinson, Acta Metall. 36 (1988) 469.

[19] Y.G. Zheng, C. Lu, Y.-W. Mai, Y.X. Gu, H.W. Zhang, Z. Chen, Appl. Phys. Lett. 88 (2006) 144103.

[20] Y.G. Zheng, C. Lu, Y.-W. Mai, H.W. Zhang, Z. Chen, Sci. Technol. Adv. Mater. 7 (2006) 812.

[21] S. Nose, J. Chem. Phys. 81 (1984) 511.

[22] W.G. Hoover, Phys. Rev. A 31 (1985) 1695.

[23] S.M. Foiles, M.I. Baskes, M.S. Daw, Phys. Rev. B 33 (1986) 7983.

[24] A.J. Cao, Y.G. Wei, Appl. Phys. Lett. 89 (2006) 041919.

[25] S. Plimpton, J. Comput. Phys. 117 (1995) 1.

[26] Y.G. Zheng, H.W. Zhang, Z. Chen, L.Wang, Z.Q. Zhang, J.B. Wang, Appl. Phys. Lett. 92 (2008) 041913.

[27] H.Q. Li, H. Choo, Y. Ren, T.A. Saleh, U. Lienert, P.K. Liaw, F. Ebrahimi, Phys. Rev. Lett. 101 (2008) 015502.

[28] F. Sansoz, V. Dupont, Appl. Phys. Lett. 89 (2006) 111901.

[29] K. Zhang, J.R. Weertman, J.A. Eastman, Appl. Phys. Lett. 87 (2005) 061921.

[30] J. Monk, D. Farkas, Phys. Rev. B 75 (2007) 045414.

**Figure captions**

Fig. 1. (a) The initial xy-plane profile of an nc-fcc copper sample created using the MC procedure; and (b) the MD model with randomly specified crystallographic orientations. The periodic cell is denoted by the dotted line in (a). Red and blue lines in (b) indicate (111) and $(11\bar{1})$ planes, respectively. Numerals 1–14 represent grain indices.

Fig. 2. Stress-strain curve for the nc-fcc copper sample under tension, where insets (a)–(h) show the microstructures at 0%, 2.5%, 3%, 4%, 5%, 6%, 12%, and 18% applied strains, respectively. The atoms in gray, green and red are those in local fcc, hcp, and disordered environments, respectively.

Fig. 3. Rotation angles of five grains with different sizes as a function of time, where numbers represent the initial diameters of these grains. Insets show those mechanisms which dominate the different plastic deformation stages and grains.

Fig. 4. Stress-assisted shrinkage of grain 8 after applied strain (a) 1%, (b) 4%, (c) 10%, and (d) 12%, in which black lines indicate the GBs.

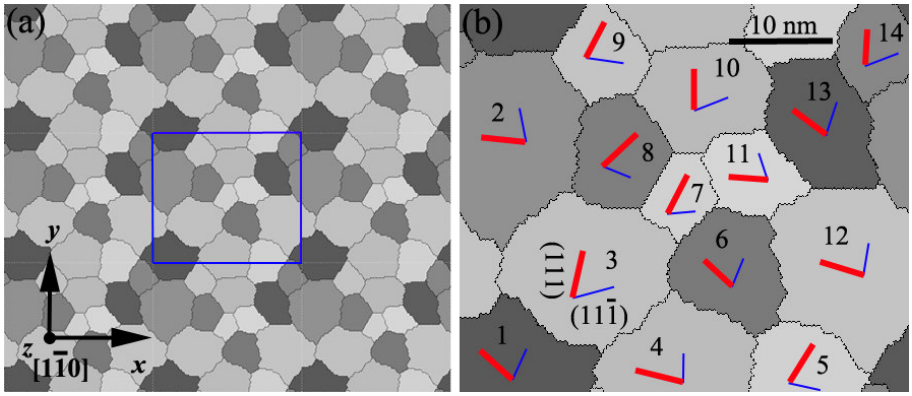


Fig. 1.

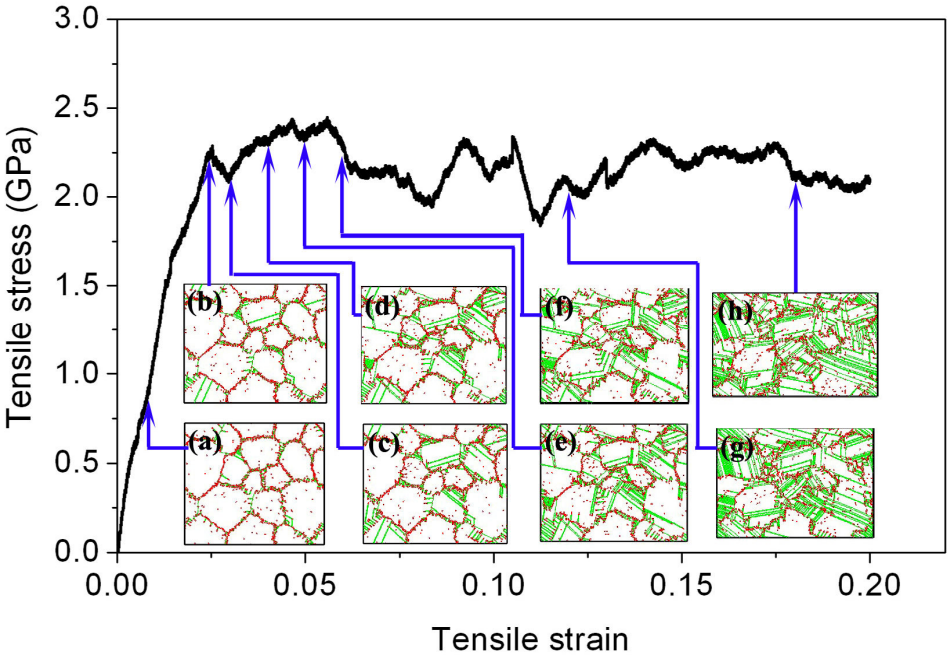
Tensile stress (GPa)
Tensile strain
3.0
2.5
2.0
1.5
1.0
0.5
0.0
0.00
0.05
0.10
0.15
0.20
(a)
(b)
(c)
(d)
(e)
(f)
(g)
(h)

Fig. 2.

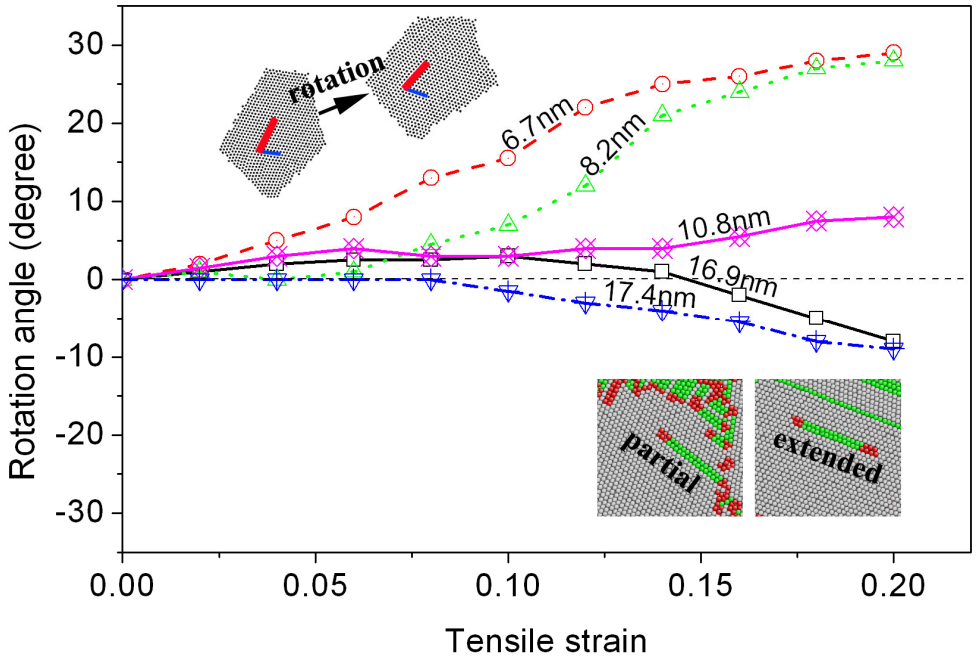
Rotation angle (degree)
Tensile strain
30
20
10
0
-10
-20
-30
0.00
0.05
0.10
0.15
0.20
rotation
6.7nm
8.2nm
10.8nm
16.9nm
17.4nm
partial
extended

Fig. 3.

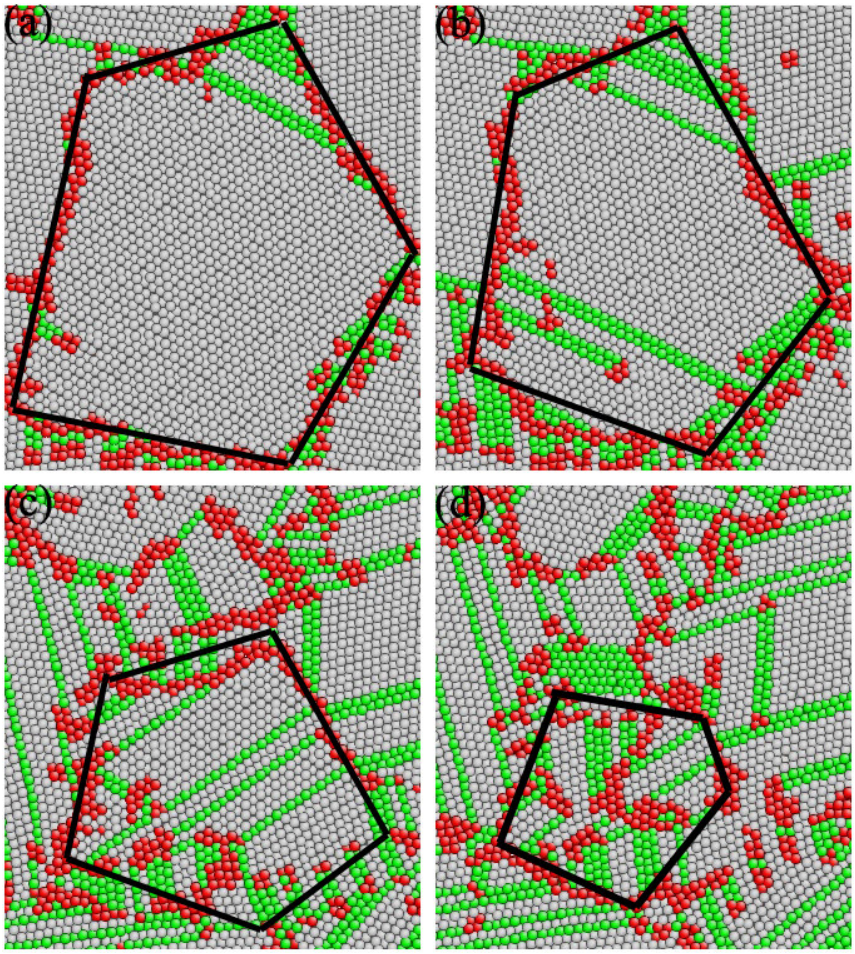


Fig. 4.